Room-temperature spintronic effects in Alq_3-based hybrid devices

V. Dediu,[1,*] L. E. Hueso,[1,†] I. Bergenti,[1] A. Riminucci,[1] F. Borgatti,[1] P. Graziosi,[1] C. Newby,[1] F. Casoli,[2] M. P. De Jong,[3] C. Taliani,[1] and Y. Zhan[4]

[1]*ISMN-CNR, Via Gobetti 101, 40129 Bologna, Italy*

[2]*IMEM-CNR, Parco Area delle Scienze 37/A, 43100 Parma, Italy*

[3]*Nanoelectronics Group, University of Twente, 7500 AE Enschede, The Netherlands*

[4]*Surface Physics and Chemistry Group, IFM, Linköping University, 58183 Linköping, Sweden*

(Received 17 June 2008; revised manuscript received 8 August 2008; published 17 September 2008)

We report on efficient spin polarized injection and transport in long (10^2 nm) channels of Alq_3 organic semiconductor. We employ vertical spin valve devices with a direct interface between the bottom manganite electrode and Alq_3, while the top-electrode geometry consists of an insulating tunnel barrier placed between the "soft" organic semiconductor and the top Co electrode. This solution reduces the ubiquitous problem of the so-called ill-defined layer caused by metal penetration, which extends into the organic layer up to distances of about 50–100 nm and prevents the realization of devices with well-defined geometry. For our devices the thickness is defined with an accuracy of about 2.5 nm, which is near the Alq_3 molecular size. We demonstrate efficient spin injection at both interfaces in devices with 100- and 200-nm-thick channels. We solve one of the most controversial problems of organic spintronics: the temperature limitations for spin transport in Alq_3-based devices. We clarify this issue by achieving room-temperature spin valve operation through the improvement of spin injection properties of both ferromagnetic/Alq_3 interfaces. In addition, we discuss the nature of the inverse sign of the spin valve effect in such devices proposing a mechanism for spin transport.

DOI: 10.1103/PhysRevB.78.115203 PACS number(s): 72.25.−b, 77.84.Jd, 85.75.−d

I. INTRODUCTION

Spin-dependent transport has been the object of intense research since the demonstration of magnetoresistive effects in metallic multilayers and magnetic tunnel junctions.[1,2] The field has evolved to the extent that commercial applications for magnetic recording and electronic memory are now available. However, achieving coherent spin transport over distances on the nanometer scale has proved difficult in normal metals and semiconductors.[3] This difficulty has motivated a search for new materials in which both efficient spin injection and transport can be realized. Among others, π-conjugated organic semiconductors (OSs) have emerged as major candidates, mainly thanks to their low spin-orbit interactions and their ability to be integrated in hybrid organic-inorganic devices.[4–6]

Spin injection into organic semiconductors was first demonstrated in lateral devices with highly spin polarized manganite $La_{0.7}Sr_{0.3}MnO_3$ (LSMO) electrodes and sexithiophene (T6) as the channel material, in which room-temperature magnetoresistance (MR) has been detected.[7] Subsequently, a spin-valve effect in vertical devices with LSMO and cobalt electrodes was observed using tris(8-hydroxyquinoline) aluminum (Alq_3) as the spin transport layer (150–200 nm thick).[8] In the latter the spin-valve effect has shown an inverse sign, indicating a higher resistivity when the magnetizations of the electrodes are oriented parallel to each other, contrary to the standard spin-valve effect.[2,3] This behavior was later confirmed in a variety of similar devices involving the simultaneous use of LSMO and Co as spin-polarized injectors.[9–11] While still puzzling, this is currently one of the most well-established results in organic spintronics.

Another important parameter of the Alq_3-based spintronic devices which is under debate is their possible operational temperature limitation. In the literature, experimental data indicate that the highest temperature for spin injection into Alq_3 is close to 250 K,[11] well below the requirement for real practical applications, where room-temperature operation is mandatory. It was also speculated that the LSMO-Alq_3-based devices have intrinsic limitations preventing room-temperature operation.[12] On the other hand, room-temperature MR has recently been reported for devices based on magnetic tunneling, in which Alq_3 was used as ultrathin tunneling layer.[13]

In this paper we present room-temperature spin injection and transport in an Alq_3-based vertical spin valve (SV) with the structure $La_{0.7}Sr_{0.3}MnO_3$/Alq_3/tunnel barrier/Co. We report on the engineering of interfaces using artificial tunnel barriers aimed at improving the efficiency of the spin injection in organic semiconductors, which guarantees a sharp definition of the organic layer thickness. We confirm the inverse spin-valve effect also for these modified geometry devices (no direct Co/Alq_3 interface) and propose a phenomenological explanation for it.

II. EXPERIMENT

$La_{0.7}Sr_{0.3}MnO_3$ films, 15–20 nm thick and with a Curie temperature of 325–330 K, were grown by pulsed plasma deposition (PPD) on matching perovskite substrates ($NdGaO_3$). This method, also called channel spark ablation, has been extensively used for the growth of various oxide films.[14,15] Alq_3 films (100–300 nm) were deposited at room temperature by organic molecular beam deposition in UHV conditions (10^{-9}–10^{-10} mbar) on LSMO thin layers. Prior to deposition the LSMO surface was reconstructed following the annealing procedures established by photoemission spectroscopy (PES) investigations.[16] Room-temperature deposi-

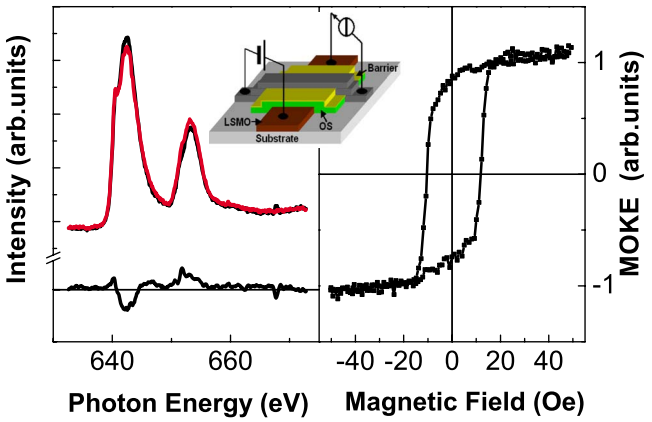

FIG. 1. (Color online) (a) Room-temperature (top) x-ray absorption spectra and (bottom) XMCD signal, which indicate surface ferromagnetism. (b) Room-temperature MOKE confirming the excellent bulk properties of the manganite films.

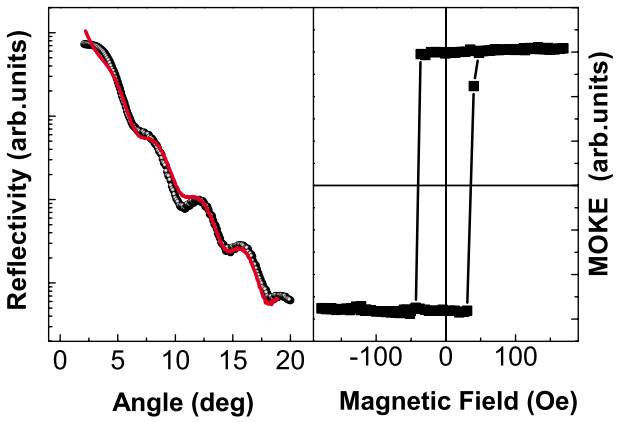

FIG. 2. (Color online) Structural and magnetic characterization of the device top electrode. (a) Room-temperature x-ray reflectivity data of a cobalt film grown on top of Alq_3/Al_2O_3. Reflectivity data allow us to certify the optimum quality of the interface. Solid line represents the fitting curve. (b) Room-temperature magneto-optical Kerr effect of a cobalt film grown on top of Alq_3/Al_2O_3, also confirming the excellent magnetic properties of the Co.

tion provides morphologically stable amorphous organic films[17,18] with molecularly flat surfaces (about 1-nm roughness). Previously we have detected spin-valve effects in devices with Alq_3 deposited at higher substrate temperature of 150 °C. In that case layers of about 100–200 nm thick were characterized by a roughness of around 10 nm.[19,20]

The Alq_3 layer is followed by 2-nm-thick Al_2O_3 or LiF tunnel barriers grown by PPD and molecular beam epitaxy, respectively. The choice of Al_2O_3 was based on its well-known properties as a tunnel barrier in magnetic tunnel junctions, while LiF barriers are extensively used in Alq_3-based organic light-emitting diodes. The top Co electrode (35 nm thick) was deposited by rf sputtering.

III. RESULTS AND DISCUSSION

Manganite films have been characterized exhaustively in order to ensure optimal device performance. In particular, special attention has been devoted to the surface magnetic properties, which are critical for the successful use of LSMO as spin injector. Although this characterization may seem routine, it is far from trivial as surface magnetization (SM) (spin polarization) should not be taken for granted even if bulk magnetic properties are excellent. Moreover, in spite of their importance, surface properties are rarely cited when dealing with manganite complex devices. In previous works we extensively examined the potential use of manganite as spin injecting contact in connection with organic semiconductors.[21,22] In particular, the LSMO postdeposition treatments have been optimized in order to recover optimal electrical and magnetic surface properties. Surface metallicity and strong circular magnetic dichroism (surface magnetization) up to room temperature were detected by PES (Ref. 21) and x-ray magnetic circular dichroism (XMCD) [Fig. 1(a)]. Magneto-optical Kerr effect (MOKE) allows us to ensure that bulk (few nanometer scale for LSMO) magnetic properties are in accordance with those published in literature [Fig. 1(b)].

We worked on the improvement of the top interface (Alq_3/Co) by introducing an inorganic tunnel barrier covering the organic semiconductor. The Alq_3/cobalt interface suffers from intrinsic limitations due to the direct deposition of the metal on top of a soft material, causing the diffusion and penetration of metal atoms in the organic layer, and a possible reaction with the organic molecules.[8] The presence of a disordered interfacial layer is preventing both efficient and especially reproducible spin injection intensity and is probably also responsible for the extremely high switching fields (100–300 mT) presented in literature.[10,23] As an example, the so-called "ill-defined layers" up to 100 nm thickness[8,11] are routinely present in literature and indicate the thickness below which the material of the top electrode penetrates in the organic layer and reaches the bottom electrode providing short circuit regime. In such a situation, a systematic Alq_3 thickness dependence of the transport properties of vertical spin valves is hardly attainable.[24]

The introduction of a thin Al_2O_3 barrier (1–2 nm thick) between Alq_3 and Co results in a sharp definition of the metal/organic interface. X-ray resonant reflectivity measurements of Co film grown on top of Alq_3/Al_2O_3 are presented in Fig. 2(a). Spectra were collected on the circular polarization beam line (ELETTRA) equipped with the IRMA reflectometer at an incident photon energy of $E=777$ eV. The spectra show interference fringes, indicating a well-defined multilayered structure with sharp interfaces. A fitting procedure based on the IMD code[25] involving a graded interface indicated an intermixing region at the interface between OS and Co as narrow as 2–3 nm. The barrier strongly limits the penetration of the Co atoms into the organic underlayer. The intermixing value we obtained is close to the intrinsic roughness of the interface, since the molecular size is close to 1 nm (full data analysis will be presented elsewhere). On similar devices without tunnel barrier, a cobalt penetration into the Alq_3 of up to 25 nm has been observed.[24] A typical magnetic hysteresis loop for the standard Co electrode grown on top of the Al_2O_3 layer measured by MOKE technique ($\lambda = 632.8$ nm) is shown in Fig. 2(b).

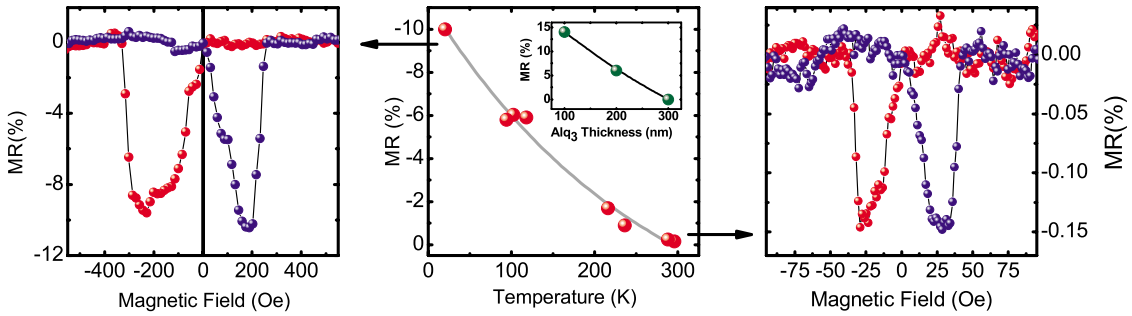

FIG. 3. (Color online) (a) Inverse spin-valve effect at 20 K showing a maximum value of 11%. (b) Magnetoresistance values as a function of temperature. The MR decreases with increasing temperature but persists up to room temperature. (c) Room-temperature inverse spin-valve effect. The magnetoresistance of each individual electrode was carefully studied, enabling us to rule out anisotropic MR as the origin of our findings. A small background nonhysteretic signal, probably intrinsic to the organic semiconductor layer, was subtracted in every case to clearly show the hysteretic spin valve effect.

Once the critical interfacial quality has been assured, we can now turn to the electrical properties of the devices. We believe that the structural improvements explained above are crucial to the enhanced device performance.

Electrical measurements of the devices (1×1 mm^2) were done in a cross-bar structure using two contacts for the bias voltage and two for the measured current. Samples were inserted in a helium exchange gas cryostat placed between the poles of a magnetic field for the temperature-dependent electrical measurements. Current (I)-voltage (V) characterizations of LSMO/Alq_3/Al_2O_3/Co devices were strongly nonlinear, indicating tunneling injection into organic electronic states.[9,19] Low-voltage resistances in the range of 1 to 10 kΩ were found for our devices, in agreement with sample geometry and organic layer thicknesses. Light-emitting effects in Alq_3 layers have been previously presented by us for both LSMO and Co electrodes.[26,27]

Under the application of a magnetic field, the spin-valve effect was detected routinely in LSMO/Alq_3/Al_2O_3/Co samples (Fig. 3). In all cases, the effect had an inverse sign, with the low-resistance state corresponding to antiparallel configuration of the two electrodes and persisted for applied voltages up to 1 V. The voltage dependence of the MR effect for this kind of devices is slightly asymmetric, and it is quite similar to what we found previously in rough Alq_3 SVs (Ref. 19). While a more detailed investigation of the thickness dependence has yet to be performed, the MR was found to decrease with increasing organic thickness (Fig. 3 inset) as it is expected for spin/charge injection into the conducting (narrow) band of the organic semiconductor and subsequent hopping toward the opposite electrode. The further reduction in the thickness of the organic layer must be accompanied by a corresponding reduction in the lateral size of the devices. With the current size, the contribution of the electrodes to the total resistance of the device is high, and therefore a thinner device would have a resistance too low to be measured reliably.

Low-temperature MR values in excess of 10% were routinely obtained on numerous devices with a 100-nm-thick Alq_3 layer (Fig. 3). Higher MR values presented by other authors[8,28] are probably caused by a lower effective thickness of the organic layer compared to the nominal one due to the so-called ill-defined layer.

In addition to a much better definition of the geometry, we remarkably achieved room-temperature operation of Alq_3-based devices as shown in Fig. 3(c). While the absolute values are still small and should be substantially improved, this provides a considerable breakthrough for the potential Alq_3 application in the field of spintronics.

The inverse spin-valve effect was also obtained in LSMO/Alq_3/LiF/Co structures, indicating that negative MR is a general feature of LSMO/Alq_3/Co devices rather than just an interface effect.[19] However, MR values for LiF were much smaller than for the Al_2O_3 case (not larger than 2%) and quickly decreasing with temperature. The reasons for such behavior are not completely clear. Nevertheless it has to be mentioned that due to chemical interactions with Alq_3 (Ref. 29), LiF, differently from Al_2O_3, is not expected to form a well-defined buffer layer. This could worsen the quality of the Co top electrode.

We should point out that the spin injection and transport in organic spin valves are radically different from those in inorganic semiconductors. This difference perhaps also holds for the conductivity mismatch problem,[30] while this aspect has yet to be investigated deeper. Indeed, many groups succeeded in injecting a spin polarized current across a direct OS/metal interface.[31] In the organic devices the two spin-polarized reservoirs (two external electrodes) are connected by a very narrow hopping channel at either the lowest unoccupied molecular orbital (LUMO) or highest occupied molecular orbital (HOMO) states, depending on interface energetics and intrinsic organic properties. Previously we have shown[32] that at the LSMO/Alq_3 interface, a 1.1-eV barrier to the LUMO level is built while the HOMO level is separated by 1.7 eV. In addition, electronic transport in this material has a mobility two orders of magnitude higher than the hole one,[33] a property well known and widely used in OLED applications. Thus, we can consider LUMO channel responsible for nearly 100% of the charge and spin transport in our devices. The LUMO channel is not represented by a real conducting band but rather by a pseudolocalized broadened level of 0.1-eV width,[34] which broadens in a Gaussian way with a standard deviation $\sigma \sim 0.35$ eV at the interface.[35] In our spin valves we first have a tunneling injection of the electrons from the LSMO into the LUMO states of Alq_3. This is followed by hopping conductivity across the "thick"

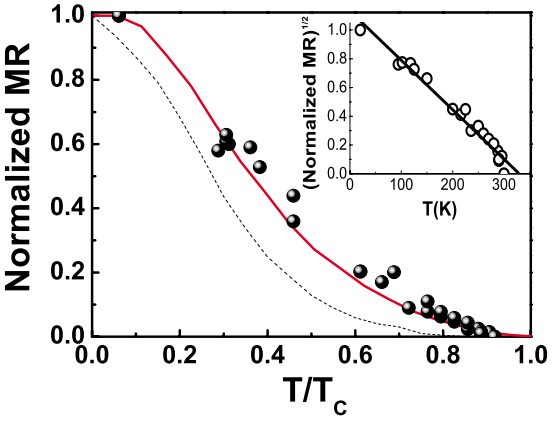

FIG. 4. (Color online) Comparison between spin-valve magnetoresistance (MR, dots), the $La_{0.7}Sr_{0.3}MnO_3$ surface magnetization (SM, solid line), and the polarized charge-carrier density (PCCD, dotted line) data from Ref. 37. Both magnitudes are plotted in reduced temperature scale normalized to the Curie temperature (T_C). The inset shows the linearized data.

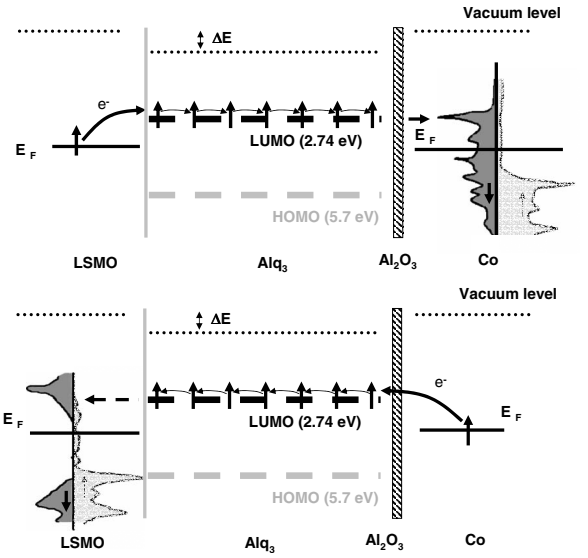

FIG. 5. Energy diagram for a $La_{0.7}Sr_{0.3}MnO_3/Alq_3$/tunnel barrier/Co organic spin valve at $V=0$ V. Upper panel: Injection of spin-up electrons from LSMO into Alq_3 and the alignment of LUMO with the Co spin-down band. Lower panel: Injection of spin-up electrons from Co through the Al_2O_3 barrier into Alq_3 and the alignment of LUMO with the LSMO spin-down band. The light gray represents the spin-up bands, while the dark gray represents the spin-down ones.

(100–200 nm) Alq_3 layer and, subsequently, once the next interface is reached, a second tunneling process moves the electron/spin from the narrow LUMO channel into the Co states through the artificial barrier.

In a recent paper[36] it has been shown that no spin-valve effect could be detected for the hole transport Alq_3-based devices of 100 nm thickness. This result is in agreement with the very low-mobility values at HOMO channel, increasing by nearly two orders of magnitude the time of flight between two spin-polarized electrodes. While the LUMO transport to 100 nm takes approximately 10^{-6} s, the HOMO transport should take about 10^{-4} s, well above the spin-relaxation times for most organic materials.[5]

The dependence of the MR with temperature (Fig. 4) is helping us to identify the critical contributions to spin transport. In Fig. 4 we can observe the normalized MR versus temperature for four independent devices with a 100-nm-thick Alq_3 layer and an Al_2O_3 barrier. The MR data are presented in square-root scale (inset) where data linearization is achieved. First, it is important to note the excellent reproducibility between the four devices. A most remarkable characteristic then is the extrapolation of data to exactly zero at the Curie temperature of the manganite, i.e., at 325 K. This allows us to draw an important conclusion—the spin transport in Alq_3 and, consequently, the spin-scattering effects are temperature independent for the investigated range of temperature. This information is extremely important for the understanding of the basic rules describing the behavior of the electrically driven spin in organic semiconductors. Figure 4 shows that our data agree very well with the SM curve for LSMO of Park *et al.*[37] The SM represents the magnetization from the top 5 Å in a standard LSMO film, as determined by spin-polarized photoemission spectroscopy[37] and it is effectively the parameter of interest for device behavior.[38]

Our results on the temperature dependence of MR are in agreement with the previous claim that the temperature dependence of MR in Alq_3 spintronic devices is governed by manganite electrode.[39] While correct in our opinion, this conclusion was not demonstrated by a straightforward data trend. Moreover the authors anticipated that room-temperature spin valve is not achievable by using the LSMO-Alq_3 combination. This conclusion was based on the fitting of MR as a function of temperature with a different surface magnetization curve.[39] The authors used the so-called polarized charge-carrier density (PCCD) (dashed curve in Fig. 4). This quantity consists of the convolution of SM and the density of states at the Fermi energy and decreases with temperature much quicker than that of SM alone. Attempts were made by the same group to circumvent the LSMO limitation and to achieve room-temperature operation for the Alq_3-based spin valves by replacing the LSMO electrode with a Fe one, which has a much higher Curie temperature.[39] Since this approach failed (the temperature behavior was even worse than for the LSMO case), the question of temperature limitations for spin injection in Alq_3 remained open.

A possible improvement on the room-temperature operation efficiency can still be achieved by the enhancement of the room-temperature surface magnetization in manganite whose nanoscale distribution is still under debate.[40,41] The replacement of the manganite electrode by materials with a higher Curie temperature requires, on the other hand, considerable efforts on the interface engineering in order to achieve efficient and reproducible spin injection intensity.

We shall discuss now the negative spin-valve effect in these and similar devices presented in literature. The existing explanation for the inverse spin-valve effect takes into account the negative (spin-down) polarization of the *d* electrons in Co and opposite (spin-up) polarization of the LSMO electrons.[8,10] While correct as far as LSMO is concerned,[42]

this simplified explanation does not take into account the possible effects of the Co *s* band, which is positively spin polarized. Moreover it has been demonstrated in a straightforward way that Co injects spin-up carriers across Al_2O_3 barrier[43–45] and even across hybrid Al_2O_3/Alq_3 barriers.[13] The sign of the MR should then be explained considering both electron currents (injected by LSMO and by Co) as spin-up currents.

While this looks apparently contradictory, the peculiar energy diagram of the full $LSMO/Alq_3/Al_2O_3/Co$ device allows us to propose a simple phenomenological model explaining the inverse spin-valve effect (see Fig. 5). The metal/Alq_3 interfacial barriers are of about 0.5–1 eV for both interfaces.[19,46] The presence of these barriers aligns the LUMO level of Alq_3 with the spin-down bands of both LSMO (Ref. 47) and Co,[48,49] considering similar Fermi energy (E_F) values for Co and LSMO (E_F=4.9–5 eV). Thus the spin-up electrons injected by either the LSMO (negative voltage) or the Co electrode (positive voltage), propagate by a hopping mechanism along the organic material where they gradually lose part of their spin polarization. Eventually, the electrons tunnel from the LUMO of Alq_3 into the spin-down bands of either the Co or LSMO electrode, respectively.

While qualitatively correct and able to justify the inversion of the spin-valve effect, the model requires operating voltages higher than 1 V, voltages at which the spin-valve effect is very weak or even absent. We cannot thus rule out a possible involvement of deep traps or impurity levels. Detailed additional investigations should be performed in order to establish precisely the spin-conducting channels in this material.

Interestingly, three (out of four) organic materials showing inverse spin-valve effect, Alq_3,[11,39] T6 (sexithiophene),[50] as well as NPB [N′-bis-(1-naphthyl)-N, N′-diphenyl-1, 1′-biphenyl-4, 4′-diamine],[39] have LUMO levels differing by less that 0.1 eV.[51] In addition, the Alq_3, which is a "pure" LUMO channel conductor, shows by far the best spintronic performances. In T6 and NPB only part of the current is transported by LUMO level.

In summary, we have achieved room-temperature operation for organic spin injection devices through control and engineering of the interfaces between organics and the spin-polarized electrodes. We believe that the improvement achieved by the introduction of tunnel barriers in organic spin valves will pave the way for future development of such devices, since we have demonstrated that the organic semiconductor does not represent any limitation in performance at least up to room temperature. This achievement is in a good agreement with the recent results from Santos *et al.*,[13] who demonstrated that in magnetic tunnel junctions the presence of a Al_2O_3 barrier increases the spin injection efficiency at the interface.

ACKNOWLEDGMENTS

The authors acknowledge Albert Fert and Pierre Seneor for the constructive criticism and discussion. We thank Federico Bona for his invaluable help in technical aspects. We also acknowledge the financial support from EU-FP6-STRP under Grant No. 033370 OFSPIN.

*v.dediu@bo.ismn.cnr.it

†Present address: Department of Physics, University of Leeds, Leeds (UK).

[1] M. N. Baibich, J. M. Broto, A. Fert, F. Nguyen Van Dau, F. Petroff, P. Eitenne, G. Creuzet, A. Friederich, and J. Chazelas, Phys. Rev. Lett. **61**, 2472 (1988).

[2] J. S. Moodera, L. R. Kinder, T. M. Wong, and R. Meservey, Phys. Rev. Lett. **74**, 3273 (1995).

[3] I. Žutic, J. Fabian, and S. Das Sarma, Rev. Mod. Phys. **76**, 323 (2004).

[4] R. H. Friend, R. W. Gymer, A. B. Holmes, J. H. Burroughes, R. N. Marks, C. Taliani, D. D. C. Bradley, D. A. Dos Santos, J. L. Brédas, M. Logdlund, and W. R. Salaneck, Nature (London) **397**, 121 (1999).

[5] V. I. Krinichnyi, Synth. Met. **108**, 173 (2000).

[6] A. R. Rocha, V. M. Garcia-Suarez, S. W. Bailey, C. J. Lambert, J. Ferrer, and S. Sanvito, Nat. Mater. **4**, 335 (2005).

[7] V. Dediu, M. Murgia, F. C. Matacotta, C. Taliani, and S. Barbanera, Solid State Commun. **122**, 181 (2002).

[8] Z. H. Xiong, D. Wu, Z. V. Vardeny, and J. Shi, Nature (London) **427**, 821 (2004).

[9] L. E. Hueso, I. Bergenti, A. Riminucci, Y. Q. Zhan, and V. Dediu, Adv. Mater. (Weinheim, Ger.) **19**, 2639 (2007).

[10] S. Majumdar, R. Laiho, P. Laukkanen, I. J. Vayrynen, H. S. Majumdar, and R. Osterbacka, Appl. Phys. Lett. **89**, 122114 (2006).

[11] W. Xu, G. J. Szulczewski, P. LeClair, I. Navarrete, R. Schad, G. Miao, H. Guo, and A. Gupta, Appl. Phys. Lett. **90**, 072506 (2007).

[12] L. G. Wang, E. Y. Tsymbal, and S. S. Jaswal, J. Magn. Magn. Mater. **286**, 119 (2005).

[13] T. S. Santos, J. S. Lee, P. Migdal, I. C. Lekshmi, B. Satpati, and J. S. Moodera, Phys. Rev. Lett. **98**, 016601 (2007).

[14] V. Dediu, J. Lòpez, F. C. Matacotta, P. Nozar, G. Ruani, R. Zamboni, and C. Taliani, Phys. Status Solidi B **215**, 625 (1999).

[15] V. Dediu, Q. D. Jiang, F. C. Matacotta, P. Scardi, M. Lazzarino, G. Nieva, and L. Civale, Supercond. Sci. Technol. **8**, 160 (1995).

[16] M. P. de Jong, V. A. Dediu, C. Taliani, and W. R. Salaneck, J. Appl. Phys. **94**, 7292 (2003).

[17] C. W. Tang and S. A. VanSlyke, Appl. Phys. Lett. **51**, 913 (1987).

[18] W. Brutting, S. Berleb, and A. G. Muckl, Org. Electron. **2**, 1 (2001).

[19] A. Riminucci, I. Bergenti, L. E. Hueso, M. Murgia, C. Taliani, Y. Zhan, F. Casoli, M. P. de Jong, and V. Dediu, arXiv:cond-mat/0701603 (unpublished).

[20] I. Bergenti, A. Riminucci, E. Arisi, M. Murgia, M. Cavallini, M. Solzi, F. Casoli, and V. Dediu, J. Magn. Magn. Mater. **316**, E987 (2007).

[21] M. P. de Jong, I. Bergenti, V. A. Dediu, M. Fahlman, M. Marsi, and C. Taliani, Phys. Rev. B **71**, 014434 (2005).
[22] M. P. de Jong, I. Bergenti, W. Osikowicz, R. Friedlein, V. A. Dediu, C. Taliani, and W. R. Salaneck, Phys. Rev. B **73**, 052403 (2006).
[23] S. Pramanik, C. G. Stefanita, S. Patibandla, S. Bandyopadhyay, K. Garre, N. Harth, and M. Cahay, Nat. Nanotechnol. **2**, 216 (2007).
[24] H. Vinzelberg, J. Schumann, D. Elefant, R. B. Gangineni, J. Thomas, and B. Büchner, J. Appl. Phys. **103**, 093720 (2008).
[25] D. L. Windt, Comput. Phys. **12**, 360 (1998).
[26] I. Bergenti, V. Dediu, E. Arisi, T. Mertelj, M. Murgia, A. Riminucci, G. Ruani, M. Solzi, and C. Taliani, Org. Electron. **5**, 309 (2004).
[27] I. Bergenti, V. Dediu, M. Murgia, A. Riminucci, G. Ruani, and C. Taliani, J. Lumin. **110**, 384 (2004).
[28] S. Majumdar, H. S. Majumdar, R. Laiho, and R. Osterbacka, J. Alloys Compd. **423**, 169 (2006).
[29] M. G. Mason, C. W. Tang, L.-S. Hung, P. Raychaudhuri, J. Madathil, D. J. Giesen, L. Yan, Q. T. Le, Y. Gao, S.-T. Lee, L. S. Liao, L. F. Cheng, W. R. Salaneck, D. A. dos Santos, and J. L. Brédas, J. Appl. Phys. **89**, 2756 (2001).
[30] G. Schmidt, D. Ferrand, L. W. Molenkamp, A. T. Filip, and B. J. van Wees, Phys. Rev. B **62**, R4790 (2000).
[31] W. J. M. Naber, S. Faez, and W. G. van der Wiel, J. Phys. D **40**, R205 (2007).
[32] Y. Q. Zhan, I. Bergenti, L. E. Hueso, V. Dediu, M. P. de Jong, and Z. S. Li, Phys. Rev. B **76**, 045406 (2007).
[33] R. G. Kepler, P. M. Beeson, S. J. Jacobs, R. A. Anderson, M. B. Sinclair, V. S. Valencia, and P. A. Cahill, Appl. Phys. Lett. **66**, 3618 (1995).
[34] M. A. Palenberg, R. J. Silbey, M. Malagoli, and J.-L. Brédas, J. Chem. Phys. **112**, 1541 (2000).
[35] M. A. Baldo and S. R. Forrest, Phys. Rev. B **64**, 085201 (2001).
[36] J. S. Jiang, J. E. Pearson, and S. D. Bader, Phys. Rev. B **77**, 035303 (2008).
[37] J.-H. Park, E. Vescovo, H.-J. Kim, C. Kwon, R. Ramesh, and T. Venkatesan, Phys. Rev. Lett. **81**, 1953 (1998).
[38] Y. Ogimoto, M. Izumi, A. Sawa, T. Manako, H. Sato, H. Akoh, M. Kawasaki, and Y. Tokura, Jpn. J. Appl. Phys., Part 2 **42**, L369 (2003).
[39] F. J. Wang, C. G. Yang, Z. V. Vardeny, and X. G. Li, Phys. Rev. B **75**, 245324 (2007).
[40] T. Becker, C. Streng, Y. Luo, V. Moshnyaga, B. Damaschke, N. Shannon, and K. Samwer, Phys. Rev. Lett. **89**, 237203 (2002).
[41] M. Cavallini, F. Biscarini, V. Dediu, P. Nozar, C. Taliani, and R. Zamboni, arXiv:cond-mat/0301101 (unpublished).
[42] E. Dagotto, T. Hotta, and A. Moreo, Phys. Rep. **344**, 1 (2001).
[43] M. Münzenberg and J. S. Moodera, Phys. Rev. B **70**, 060402(R) (2004).
[44] E. Y. Tsymbal, O. N. Mryasov, and P. R. LeClair, J. Phys.: Condens. Matter **15**, R109 (2003).
[45] R. Meservey and P. M. Tedrow, Phys. Rep. **238**, 173 (1994).
[46] Y. Q. Zhan, M. P. de Jong, F. H. Li, V. Dediu, M. Fahlman, and W. R. Salaneck, Phys. Rev. B **78**, 045208 (2008).
[47] J. M. Pruneda, V. Ferrari, R. Rurali, P. B. Littlewood, N. A. Spaldin, and E. Artacho, Phys. Rev. Lett. **99**, 226101 (2007).
[48] E. Y. Tsymbal and D. G. Pettifor, J. Phys.: Condens. Matter **9**, L411 (1997).
[49] P. K. de Boer, G. A. de Wijs, and R. A. de Groot, Phys. Rev. B **58**, 15422 (1998).
[50] V. Dediu, A. Riminucci, I. Bergenti, L. E. Hueso, C. Newby, C. Taliani, and F. Casoli (unpublished).
[51] A. Kahn, N. Koch, and G. Weiying, J. Polym. Sci., Part B: Polym. Phys. **41**, 2529 (2003).